Journal of Cellular Biochemistry 30:227-243 (1986)
Membrane Skeletons and Cytoskeletal-Membrane Associations 113-129

Fine Structure of Gels Prepared From an Actin-Binding Protein and Actin: Comparison to Cytoplasmic Extracts and Cortical Cytoplasm in Amoeboid Cells of *Dictyostelium discoideum*

J.J. Wolosewick and John Condeelis

Department of Anatomy, University of Illinois at Chicago, Chicago, Illinois 60612 (J.J.W.) and Department of Anatomy and Structural Biology, Albert Einstein College of Medicine, Bronx, New York 10461 (J.C.)

We have identified the three-dimensional ultrastructure of actin gels that are formed in well-characterized cell extracts and mixtures of purified actin and the 120K actin-binding protein and compared these to the ultrastructure of the cytoplasmic matrix in regions of nonextracted *Dictyostelium* amoebae that are rich in actin and 120K. This ultrastructural characterization was achieved by using critical-point-dried whole-mount preparations.

All three preparations—gelled extracts, purified proteins, and cortical cytoplasm—are composed of filament networks. The basic morphological feature of these networks is the presence of contacts between convergent filaments resulting in "T" or "X" shaped contacts.

The finding that actin-containing gels are composed of filament networks, where the primary interaction occurs between convergent filaments, reconciles the known requirement of F actin for gelation with the amorphous appearance of these gels in thin sections.

Increasing the molar ratio of 120K dimer to actin monomer increases the number of contacts between filaments per unit volume and decreases the lengths of filaments between contacts. This indicates that 120K stabilizes interactions between filaments and is consistent with biochemical evidence that 120K cross-links actin filaments.

The cortical network in situ resembles more closely networks formed in 120K-rich extracts than networks assembled in mixtures of purified 120K and actin. The heterogeneity of filament diameters and variation of network density are properties shared by extracts and the cytomatrix in situ while networks found in purified 120K-actin gels have filament diameters and densities that are more uniform. These differences are certainly due to the more complex composition of cell extracts and cortical cytoplasm as compared to that of purified 120K-actin gels.

Received April 16, 1985; revised and accepted October 14, 1985.

Key words: actin gelation, amoeboid movement, cortical cytoskeleton

Although the form and function of actin-containing structures in muscle cells have been elucidated, the form, distribution, and function of this abundant protein in nonmuscle cells in vivo and in culture are understood less clearly.

The striking and elegant images derived from fluorescence microscopy have been useful in identifying the general distribution of actin-containing structures within cells. Fluorescently labeled heavy meromysin or antibodies directed against actin and 7-nitrobenz-2oxa-3diazole (NBD) phallacidin have been used to demonstrate that stress fibers contain actin [1,9,16,31]. However, fluorescence microscopy is limited by the resolving power of the microscope such that individual filaments comprising stress fibers are not visualized by this technique. Furthermore, the structure of actin that is not contained within stress fibers, which apparently accounts for the so-called background diffuse fluorescence in the cytoplasm, also is not resolved by fluorescence microscopy.

Transmission electron microscopy of conventional samples (that is, thin sections of epoxy-embedded cells) permits the resolution of the 7 nm diameter filaments comprising stress fibers and, in principle, the more diffuse filamentous structures in the cytoplasm. Transmission electron microscopy and decoration with subfragments of myosin permit direct identification of the actin-containing filaments in these structures [14]. However, the restricted sample size (60 nm thick sections) and electron scattering by the resin make it difficult to obtain more detailed information regarding the three-dimensional organization of diffuse filamentous structures.

Examination of resinless samples, ie, those not filled by an electron-scattering resin (eg, Epon) has been of practical value in providing more easily interpretable three-dimensional information on cell fine structure. These specimens have included whole cultured cells fixed and critical-point-dried, frozen-dried, frozen-substituted [21,28,29], resinless sections of cells [10,26,27], and replicas of fast-frozen deep-etched cells [12]. In conjunction with stereo-tilt, the three-dimensional information derived from these samples is extremely valuable in determining the spatial relationships of the diffuse filamentous components of the cytoskeleton.

From these studies, an extensive cytoplasmic filament network has been visualized that interconnects the major cytoskeletal and membranous organelles. This network has been termed the microtrabecular lattice [28,29] and, more recently, the cytoplasmic matrix [36].

The extent to which actin comprises the various filamentous structures in the cytoplasmic matrix is currently unknown. Some investigators have approached this problem by using detergent extraction of chemically fixed cells to maintain the cytoplasmic matrix intact and accessible so that its composition could be investigated with various cytochemical probes. Studies with probes for actin have demonstrated that at least some of the filaments in the residual cytoplasmic matrix contain actin [32].

The concept that actin is a major component of the cytoplasmic matrix is also anticipated by the finding that nonmuscle cells contain proteins that bind to and gel F actin [33], a phenomenon that may be responsible for dramatic changes observed in cytoplasmic consistency in motile cells [24]. The physiology of actin gelation has been studied most extensively in cell extracts in which it is found that the major components of the gel are actin and actin-binding proteins [5,15,20,23]. Further-

more, conditions that affect actin gelation in cell extracts such as temperature, Ca^{++}, ATP, and pH [5] are also found to vary the consistency of the cytoplasm in intact cells [24] and the morphology of the cytoplasmic matrix in situ [18].

In this investigation we sought to answer two questions regarding the role of actin in assembling the cytoplasmic matrix. First, what is the three-dimensional ultrastructure of actin gels that are formed in cell extracts of *Dictyostelium*, and mixtures of purified actin and the 120K actin-binding protein from *Dictyostelium*? Second, is the three-dimensional ultrastructure of these actin gels similar to that of the cytoplasmic matrix in regions of *Dictyostelium* amoebae that are rich in actin and 120K? To answer these questions, we have observed resin-free samples in stereo tilt using conventional and high-voltage electron microscopy (HVEM).

MATERIALS AND METHODS

Cells

Amoebae of *Dictyostelium discoideum* strain AX3 were grown in axenic culture [17] and harvested while in log growth phase at a concentration of ca. 7×10^6/ml.

Preparation of Extracts and Proteins

The nonmotile cell extract "SB" was prepared as described [5] with the following modification: Cells were homogenized in 2 volumes of 0.5M sucrose, 5 mM DTT, 0.5 mM ATP, 10 mM Tris-HCl, 5 mM Pipes, 7.5 mM EGTA, 2 mM EDTA, 0.06 ml trasylol/ml, 0.3 mg/ml trypsin inhibitor, and 2 mM PMSF at pH 7.0 and the homogenate was clarified for 1 hr at 100,000g. This modification decreased the amount of proteolysis of the actin-binding proteins. The supernatant was treated as S3 in our previous procedure for the preparation of SB [5]. The 120K protein [4] and *Dictyostelium* actin [34] were isolated as described elsewhere. Rabbit muscle actin was isolated according to Spudich and Watt [22].

Electron Microscopy

Cells. Cells were harvested at 200g—5 min, washed in 20 mM KCl, 0.7 mM $CaCl_2$, 2 mM $MgSO_4$, 40 mM sodium phosphate pH 6.4. The cells were plated out and allowed to spread on polylysine- (0.1%) treated formvar and carbon-coated gold grids [30] or onto 35 × 10-mm plastic petri dishes. The degree of spreading of the cells was monitored by phase contrast microscopy. The cells were fixed within 30 min after plating in 2% glutaraldehyde in 40 mM sodium cacodylate, pH 7.0 for 20 min, washed twice in 40 mM sodium phosphate pH 6.0, and exposed to osmium tetroxide (1% in 40 mM sodium phosphate pH 6.0) for 5 min, and washed in distilled water.

The cells on gold grids were processed as follows. The grids were removed from the coverslips, transferred to a multiple grid holder, dehydrated, and dried by the critical-point method. The grids were coated with carbon and stored desiccated over silica gel until observation in the high-voltage electron microscope at the University of Colorado, Boulder.

Proteins. A solution of purified 120K (Fig. 1B) at approximately 1 mg/ml was dialyzed against 2 mM $MgSO_4$, 5 mM EGTA, 1 mM $CaCl_2$, 10 mM Pipes, 0.1 M KCl, 1 mM EDTA, and 0.5 mM DTT pH 7.0 and used in the experiments described below. G actin or a mixture of G actin and 120K were placed on formvar- and carbon-

coated grids held on glass coverslips. The coverslips were placed in a moist chamber consisting of four layers of moistened paper in the bottom of a sealable plastic box. Final actin concentration on the grids was 0.8 mg/ml while the 120K concentration was varied to achieve the molar ratios to actin shown in Table I. Protein solutions were held at room temperature for 15 min to permit polymerization of the actin. Gelation time of identical 120K-actin mixtures was measured in a falling ball viscometer [19]. Gelation usually occurred within 2 min at room temperature.

Grids were fixed in preparation for critical-point drying. Fixation was carried out using several different methods: (1) Proteins were fixed by addition of a drop of 2% glutaraldehyde or 5% formaldehyde, 40 mM sodium cacodylate pH 7.0 for 10 min, rinsed with water, and stained with buffered 1% O_SO_4 or 1% uranyl acetate for 1 min. (2) Proteins were fixed for 10 min with vapors of formaldehyde generated by heating paraformaldehyde in a moist chamber. (3) Coverslips were floated grid side down in 2% glutaraldehyde, 50 mM sodium cacodylate pH 7.0 in a 35 × 10 mm petri dish for 10 min. Fixative was exchanged with distilled water and then 1% uranyl acetate without disturbing the grid surface.

The method of fixation had no effect on the fine structure of the 120K-actin gel, although method 1, which employed staining with 1% O_SO_4, resulted in unpredictable damage to the preparations of pure F actin. All of the results shown in this paper were obtained with method 3, which employed no O_SO_4.

After fixation and staining, the grids on coverslips were transferred to a large vessel filled with distilled water and individual grids were placed in a brass grid holder, dehydrated in ethyl alcohol, and dried from carbon dioxide by the critical-point method. The grids were subsequently coated on both sides with a thin layer of carbon and stored desiccated over silica gel until ready for viewing in the high-voltage electron microscope. Latex spheres that had been dialyzed against the same buffer as 120K were added to the cell-free extracts before polymerization (eg, Fig. 2), in order to aid in locating the preparations on the grids. These spheres had no effect on the polymerization or gelation of the proteins, nor were they found essential in locating the gels, and their use was discontinued. Gels of 120K-actin that were to be embedded in epoxy were prepared as described above and fixed in 2% glutaraldehyde in 50 mM sodium cacodylate, pH 7.0 for 30 min, washed in distilled water, and stained in aqueous 0.5% uranyl acetate for 3 min. The gels were dehydrated in ethyl alcohol, infiltrated, and embedded in Epon. Sections (70–100 nm) were cut with diamond knives on an MT-2 ultramicrotome, mounted on uncoated 300-mesh grids, stained with 4% aqueous uranyl acetate for 20 min, washed, dried, and viewed in the Jeol-100 CX electron microscope operated at 100 kV.

MEASUREMENTS

Electron micrographs of critical-point-dried F actin and 120K-actin gels were taken at initial magnifications of 50,000×. These were subsequently printed (without identification) to a final magnification of 125,000. The electron micrographs were aligned and viewed in stereo using a 9 × 9-inch stereoviewer. A 1 μm^2 area was marked on each stereo pair and the number of contacts in this area was determined. Five such areas were counted for each preparation. Filament contacts were identified in stereo as X- and T- (or Y-) shaped intersections. There were also more complex contacts where many filaments converged into a single contact (Fig. 7). These were

counted as a single contact. Lateral interactions between filaments were also scored as a single contact. The lengths of the filaments connecting adjacent contacts and the depth of the preparation was determined by parallax [35]. The number of contacts that was counted in 1 μm^2 of each stereo pair was converted to μm^3.

RESULTS

Ultrastructure of the Actin Gel in Cell Extracts

The structure of actin gels formed in extracts of *Dictyostelium* amoebae was examined previously by conventional negative-staining and thin-section techniques [5]. It was demonstrated that the gels were composed of an amorphous aggregate that contained actin filaments that bound heavy meromyosin. However, the detailed fine structure of the amorphous gel was so difficult to discern by conventional electron microscopy of epoxy sections that the extent to which actin was filamentous in the gel, before heavy meromyosin decoration, was questioned seriously [5].

In order to evaluate the detailed fine structure of actin gels formed in cell extracts of *Dictyostelium discoideum*, we prepared myosin-free extracts (SB fraction) as described above. This extract exhibits Ca^{++}-sensitive gelation but will not exhibit ATP-dependent contraction in the absence of exogenous myosin since it has been depleted of its endogenous myosin [5]. The composition of the extract is shown in Figure 1. The extract contains actin-binding proteins that measure 250,000 [37], 120,000 [4], and 95,000 [7] daltons in SDS and actin as well as a number of unidentified components. The major actin-binding protein in these extracts is the 120,000-dalton protein (120K) that we have purified [4] and used in the study reported here. This protein has substantial actin gelling activity [25].

When the cell extract is gelled on an electron microscope grid, fixed, and critical-point-dried, it is possible to view the ultrastructure of the entire thickness of gel in the HVEM in stereo-tilt (Fig. 2). This technique demonstrates that the gelled extract is composed of filaments that range in diameter from 4 to 12 nm. The filaments are arranged as both networks and filament bundles (Fig. 2, arrows). The major portion of the gelled extract is composed of a filament network as shown at high magnification in Figure 3. The filaments within the networks form numerous contacts with each other. The frequency of and distance between contacts differ from place to place in the network, demonstrating that the density of the gel varies (Fig. 3).

Ultrastructure of 120K-Actin Gels

We next investigated the morphology of gels prepared from purified actin and the 120K protein. The 120K protein was chosen for these studies because it is the major actin-gelling protein present in the cell extracts and it is concentrated in the cell cortex of *Dictyostelium* amoebae [6,34]. Actin from either rabbit skeletal muscle or *Dictyostelium* amoebae was used in these studies (Fig. 1C,D). The results were not influenced by the source of the actin.

In order to determine what effect 120K had on gel morphology, we constructed gels by mixing 120K and G actin together with different molar ratios. All of the preparations containing 120K formed gels of varying rigidity when actin was polymerized, while purified actin did not form a rigid gel at the concentrations used in these experiments. However, for comparison, solutions of F actin were applied to the grids, fixed, and critical-point dried as were gelled preparations containing 120K. By

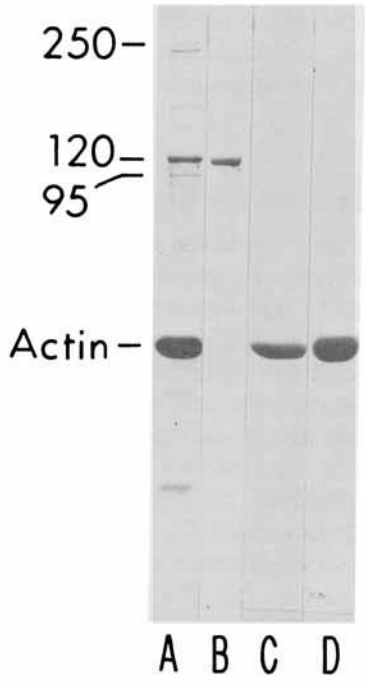

Fig. 1. SDS polacrylamide gels of (A) cell extract SB; B) 120,000-dalton actin binding protein from *Dictyostelium*; C) actin isolated from rabbit skeletal muscle acetone powder; D) actin isolated from *Dictyostelium* amoebae.

applying a protein solution as a very thin layer on the grid surface, it was possible to maintain the solution on the grid as a stable film during fixation, staining, and drying. In this way we generated preparations of gelled 120K-actin and ungelled F actin of similar thickness for direct comparison.

The results of these experiments are shown in Figures 4–8 and are summarized in Table I. Figures 4 and 6 show preparations of purified F actin. The filaments are approximately 8 nm in diameter, but some appear thicker at low magnification due to lateral association between 8-nm filaments. Most of the contacts occur between filaments converging at low angles to each other. There are few high-angle, ie, X- or T-shaped, contacts.

Figures 5 and 7 show 120K-actin gels prepared at a molar ratio of 1/30 (120K dimer:G actin). The 120K-actin gel is composed of a network of filaments that resembles that formed from pure actin when viewed at low magnification. However, close observation demonstrates that the 120K-actin gel contains, on average, a larger number of filament contacts, most contacts are X- and T-shaped and lengths of filaments connecting contacts are shorter than in preparations of pure actin. The individual filaments in the 120K-actin gel are thicker, averaging 12 nm in diameter, and there are fewer lateral interactions between filaments. There are no filament bundles similar to those seen in the cell extracts.

In order to determine the extent to which the density of the network increased with increasing molar ratios of 120K/actin, we measured the number of filament

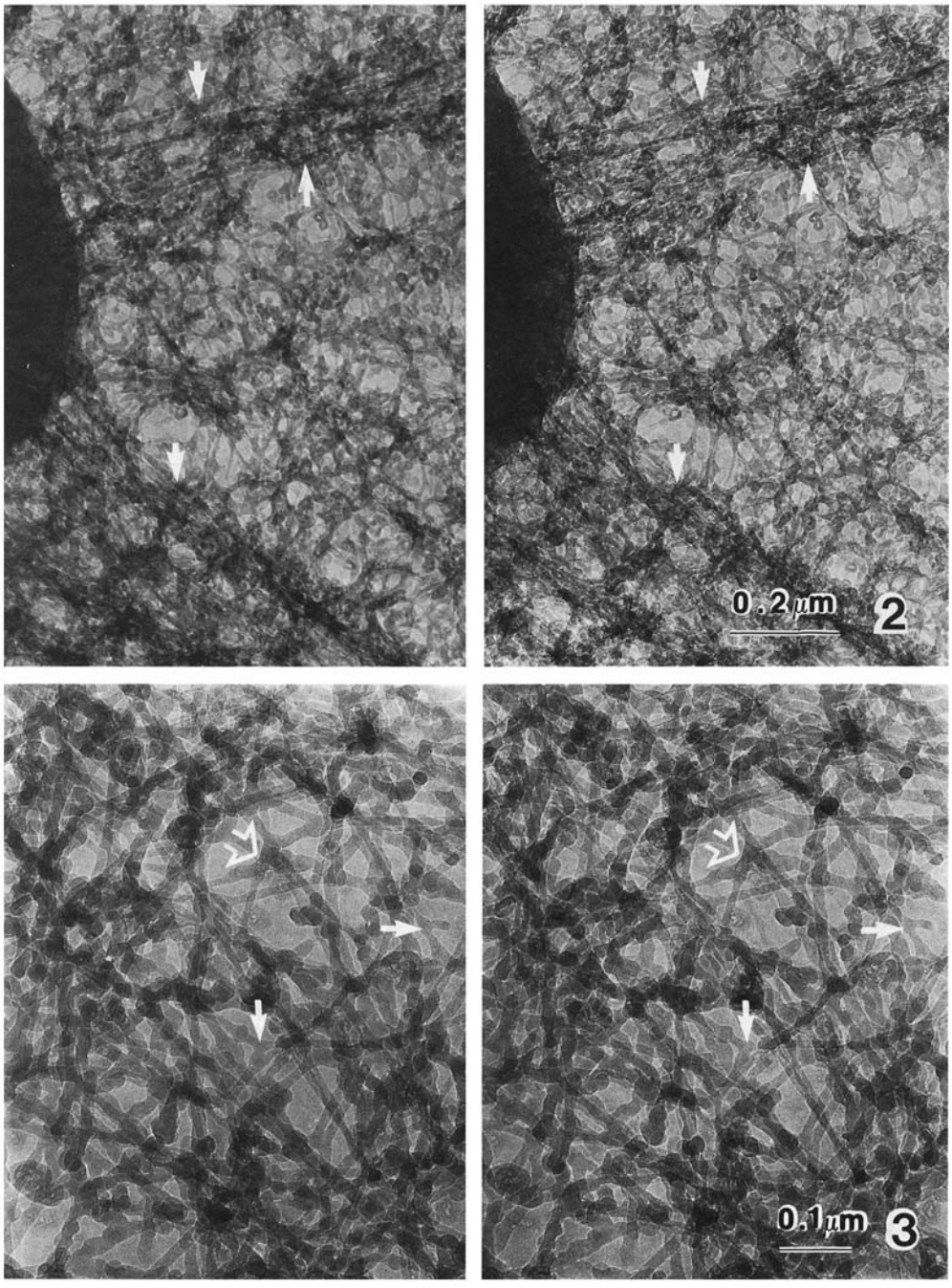

Fig. 2. Stereo image of the gel formed in extract SB with the composition shown in figure 1A. This stereo image demonstrates the presence of numerous short filaments (4–12 nm in diameter). Bundles are also found that form from the lateral association of microfilaments (arrows). 6° total tilt.

Fig. 3. High magnification of the filament network in gelled SB. T- (arrows) and X-shaped contacts are common. Complex focal contacts (open arrows) involving many filaments are also present. 4° tilt.

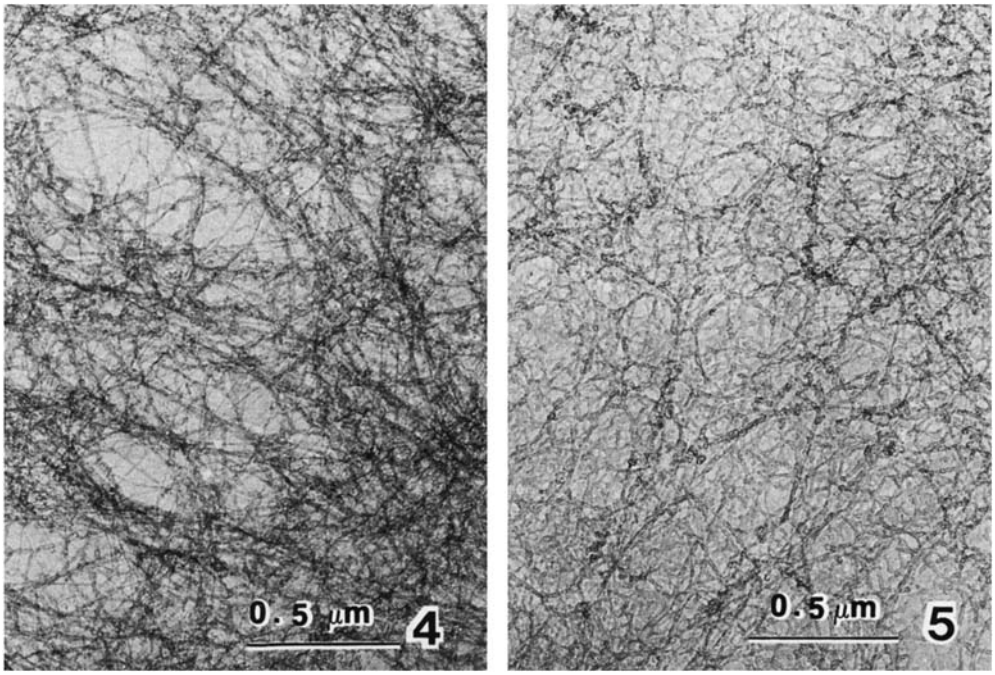

Fig. 4. Purified F actin after critical-point drying at low magnification. The density of the preparation varies and many of the filaments are 1 μm in length or greater.

Fig. 5. The 120K-actin gel at a molar ratio of 1/30 after critical-point drying at the same magnification as Figure 4.

TABLE I. Effect of 120K Protein on Gel Morphology

Molar ratio 120K dimer:G actin	No. of contacts/μm^3	Range of filament lengths between contacts (μm)
0	298 ± 129	0.05–2.0
1/80	980 ± 109	0.05–1.7
1/30	1,581 ± 274	0.04–0.4
1/15	2,908 ± 640	0.02–0.06

contacts per μm^3 and the range of filament lengths between contacts. As shown in Table I, there was a marked increase in the number of filament contacts per μm^3 and a decrease in the range of filament lengths between contacts with increasing molar ratios of 120K/actin.

In order to determine if the dense network seen in critical-point-dried whole-mounted gels was a property of the 120K-actin interaction and not the result of critical-point drying, 120K-actin gels were prepared for transmission electron microscopy of conventional thin epon sections. A thin section of a 120K-actin gel that was embedded in epoxy is shown in stereo in Figure 8. The molar ratio of 120K to actin is 1/40. Even in a thin section, a filament network is observed. However, the random orientations of the filaments result in a discontinuous, amorphous morphology that is characteristic of unstretched, gelled extracts viewed in thin section [5].

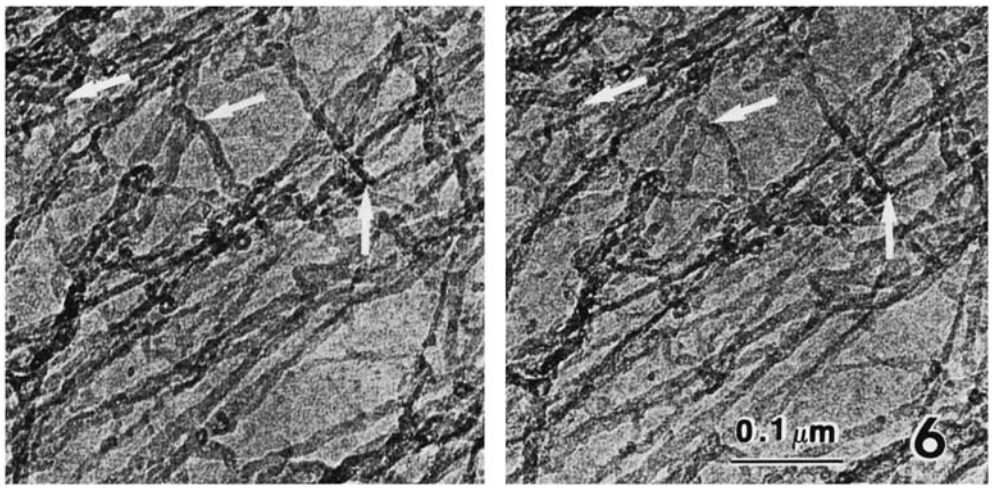

Fig. 6. Stereo pair of purified F actin. A typical region showing how the filaments tend to align to make low-angle contacts. A few X- or T-shaped contacts are seen (arrows). Many of the filaments are quite long and can be followed for at least 0.4 μm as they cross the field of view. 5° total tilt.

Morphology of the Cortical Cytoplasmic Matrix

In order to compare the three-dimensional ultrastructure of actin gels formed in vitro to that of the cytoplasmic matrix in regions of the cell that are rich in 120K and actin, amoebae were prepared for HVEM by the same fixation and critical-point drying protocol used above for the gels.

Amoebae were permitted to spread and locomote on glass or plastic substrates treated with poly-L-lysine. Cells were fixed as described above and viewed as whole mounts in either the scanning electron microscope, or in the HVEM. The quality of fixation and general morphology of the cells are shown in Figure 9. When cells are permitted to locomote on these surfaces, they send out extensions of the cell cortex called lamellipodia or pharopodia. Cells also show extensive ruffling of the cortex in regions where phagocytosis is either occurring or is imminent, as seen during the process of yeast ingestion in Figure 9a. During net locomotion, one of these pharopodia will become dominant at the leading edge of the cell, as shown in Figure 9b. This structure will often persist and may expand to form a more rounded pseudopodium (Fig. 9c).

Ruffles, pharopodia, and pseudopodia are all filled with a dense network of filaments. The network is dense enough to give the impression that it excludes the membrane-enclosed organelles from these structures. Deep to this area, the network is open and much less dense (Fig. 9b). This is the region of the cytoplasm where membrane-enclosed organelles are observed to soltate in living cells.

During locomotion, these cells remain too thick (5–10 μm) in the cytoplast for detailed study of the cytoplasmic matrix even with the HVEM. Further analysis of the cytoplast will have to await the use of resinless sectioning techniques (eg, PEG [26,27], or freeze-fracture, deep-etch [12]). However, the morphology of the cytoplasmic matrix can be studied at high magnification in ruffles and pharopodia that are

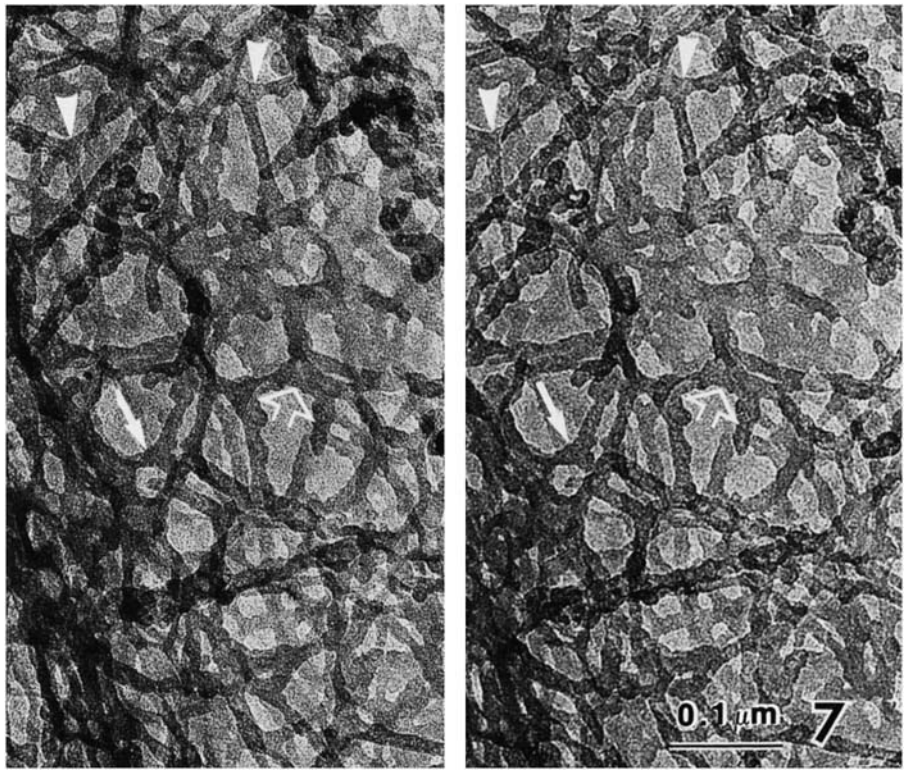

Fig. 7. The 120K-actin network at a molar ratio of 1/30. Such preparations contain numerous T- (arrows), and X- (arrowheads) shaped contacts. Complex foci (open arrow) are also present. These were scored as a single contact in Table I. The lengths of filaments connecting contacts are relatively short compared to F actin preparations. 9° tilt.

thin enough in whole mount preparations to permit penetration by the electron beam. These are the regions of the cell that contain concentrations of 120K and actin [6,34].

As shown in Figures 10 and 11, the cell cortex is filled with a three-dimensional network of filaments that make numerous contacts with each other often forming T- or X-shaped interactions. The morphology of the cortical network resembles filament networks that are found in vitro in the cell extracts. The filaments have diameters that range from 3 to 12 nm and the density of the network varies dramatically. Many complex foci are present and in some regions the density of the cytomatrix is too great to permit resolution of detail. One striking difference between the cortical network in situ and the structure of gelled extracts in vitro is the absence of filament bundles from the cortical network.

Many of the thinner filaments in the network immediately adjacent to the cell membrane make contact with the cytoplasmic surface of the membrane (Fig. 10). It is difficult, due to the density of the cortical network, to decide whether these contacts represent the lateral or end-on type attachments described previously [38].

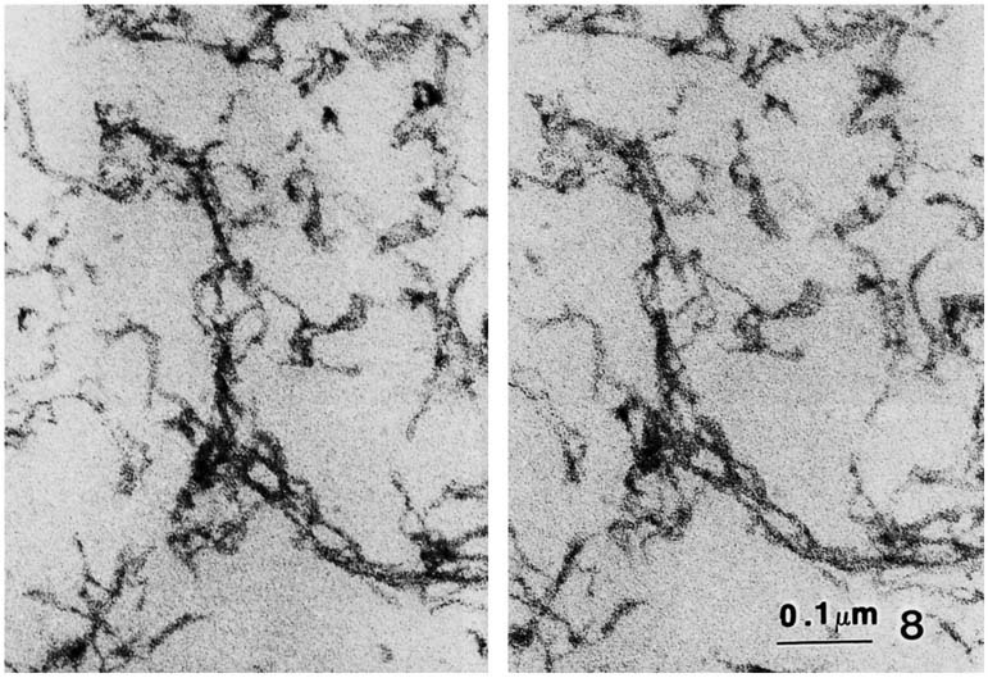

Fig. 8. Stereo image of a thin section of the 120K-actin network prepared with a molar ratio of 1/40. As in stereo images of critical-point-dried gels, numerous filament contacts are visible. Due to the limited depth of field, many filaments are only partially included within the plane of section, giving the gel a discontinuous and amorphous appearance. 30° tilt.

DISCUSSION

Morphology of Actin Gels Formed In Vitro

Electron microscopy of whole, critical-point dried, gelled extracts and 120K-actin mixtures demonstrates that these gels are composed of networks of microfilaments. The basic morphological feature of these networks is the presence of contacts between convergent filaments that are at large angles to each other so that each contact represents only a short overlap between filaments (ie, X- or T-shaped). Lateral associations between aligned filaments are also observed for short distances, but fewer of these interactions are observed in comparison to preparations of purified F actin. The filaments in 120K-actin networks appear to disperse and would be expected to fill a larger volume than that occupied by an equal mass of bundled filaments.

A network morphology is also found in preparations of purified F actin. However, the number of contacts between filaments per unit volume is smaller and the frequency of lateral interactions between filaments is greater than in 120K-actin networks. Furthermore, very few X- or T-shaped contacts are observed in preparations of F actin.

The ultrastructure of gelled extracts is more complex than preparations of either purified F actin or 120K-actin. The gelled extracts contain extensive networks that

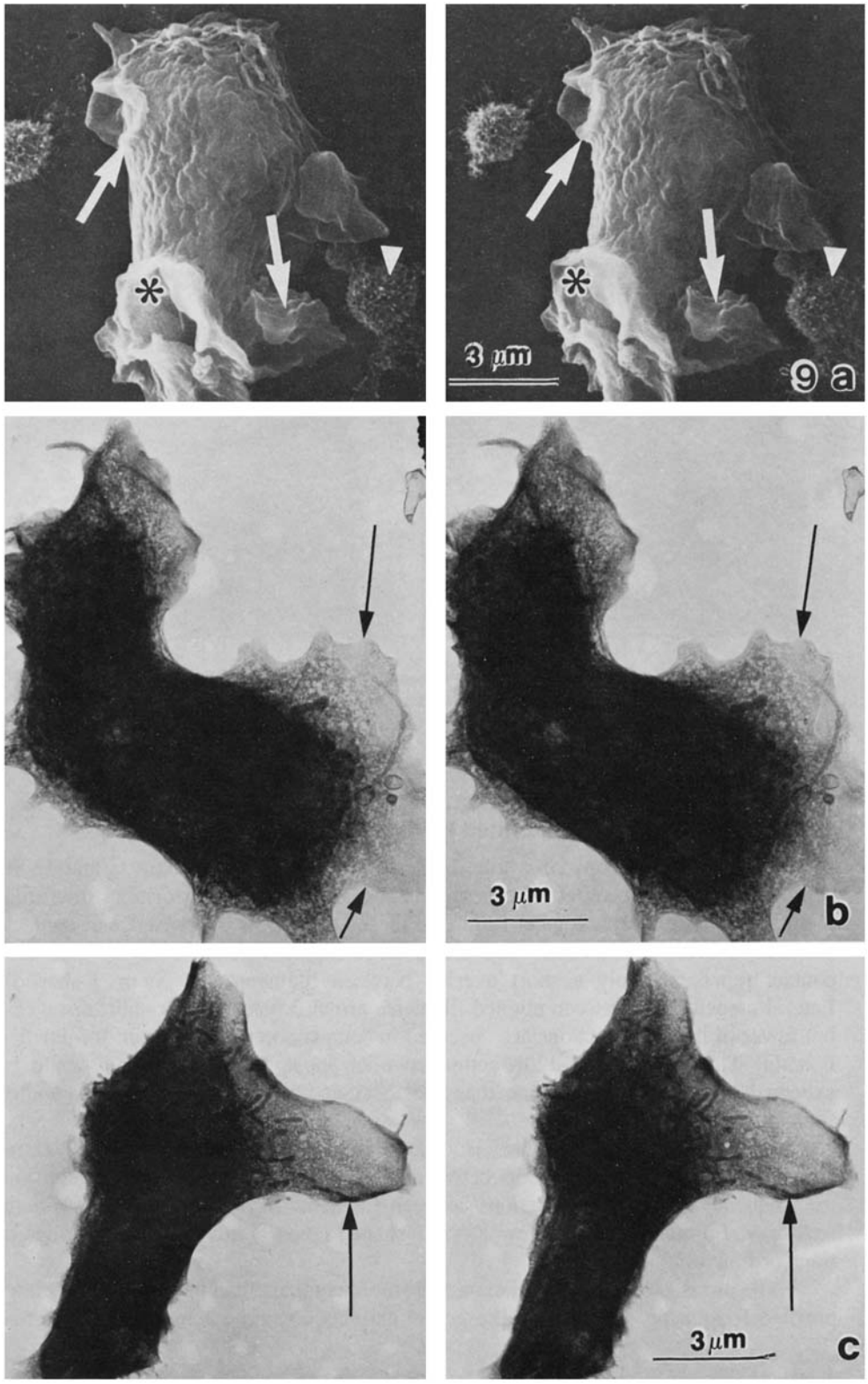

Fig. 9

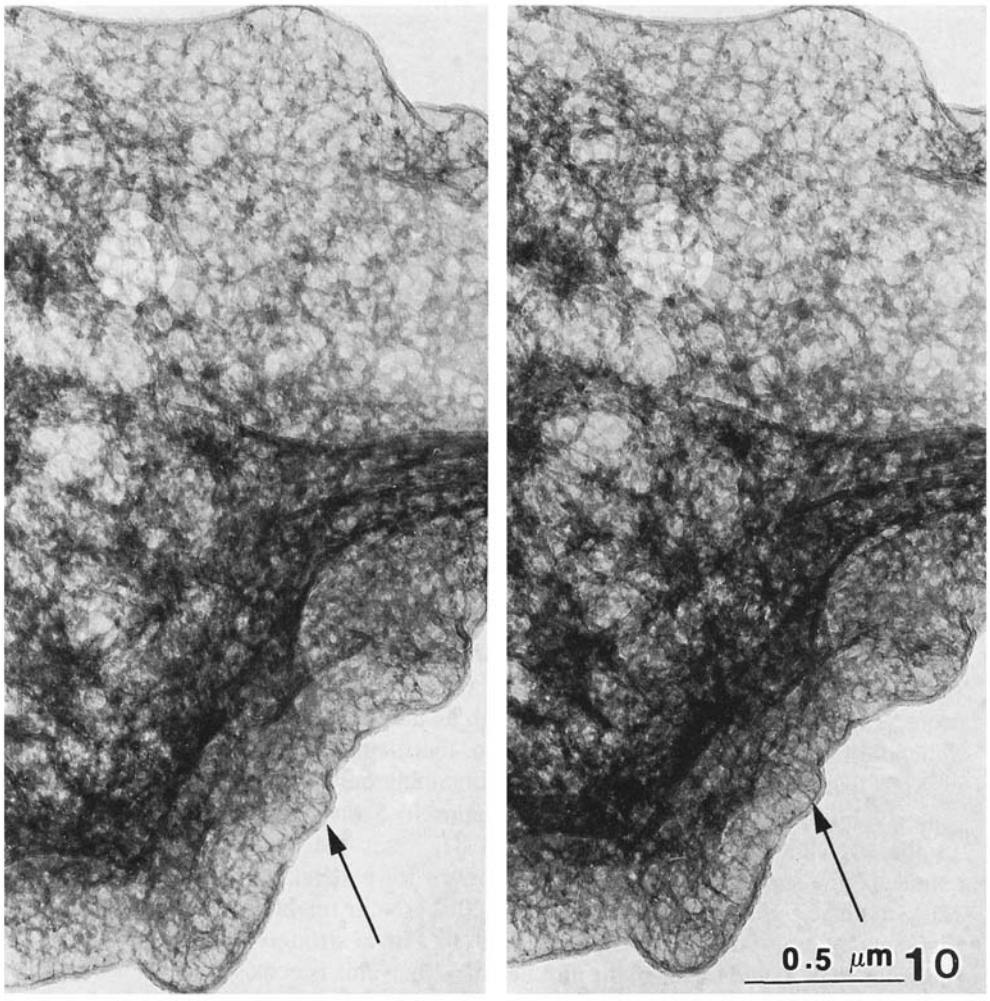

Fig. 10. Stereo image of a portion of a pharopodium from a critical-point-dried amoeba observed with the HVEM. The network in the pharopodium is continuous throughout the cytoplasm. Numerous filaments appear to make contact with the plasma membrane (arrows). 10° total tilt.

Fig. 9. (a) Stereo scanning electron micrograph of a whole critical-point-dried amoeba fixed during locomotion. This image shows the lamellar extensions of the cell surface that form food cups (arrows) during ingestion of a yeast cell (arrowhead). Lamellipodia are found at the leading edge of the cell (asterisk). (b,c) Stereo transmission electron micrographs of whole critical-point-dried amoebae fixed during locomotion. The pharopodia (b, arrows) and pseudopodia (c, arrow) are filled with a dense filament network. The magnification is too low here to observe the network in detail, although the zone of exclusion in the pharopodium is seen easily. 10° total tilt. These transmission images were photographed on the 1,000-kV electron microscope.

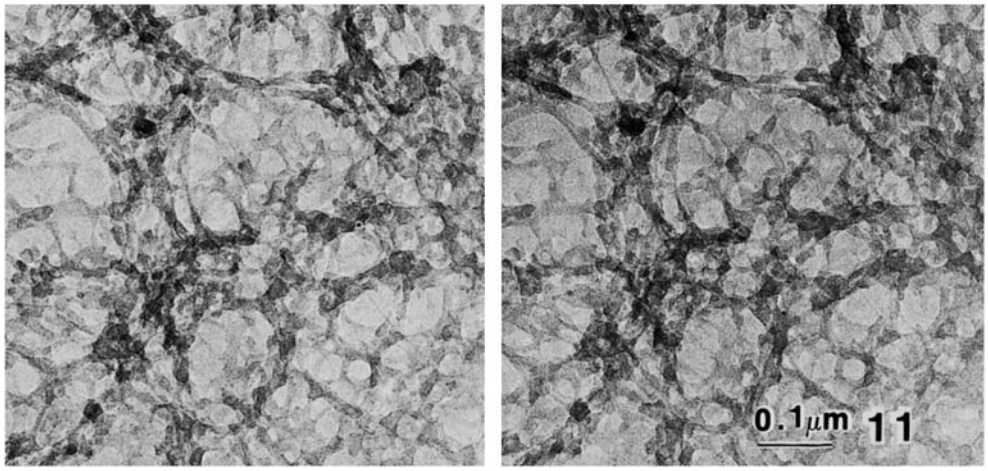

Fig. 11. Higher-magnification stereo image of a region of the cortical network more distal to the plasma membrane showing filament contacts in more detail. Tilt 6°.

are quite similar to those in preparations of 120K-actin with large numbers of contacts and few lateral associations. However, extracts contain large filament bundles interspersed among the networks. Bundling may be caused by additional actin-binding proteins that are present in the extract, such as the 95K protein that has been shown to bundle filaments in vitro. [7]. In addition, the filament diameters are more heterogeneous than those found in preparations containing only 120K and actin.

Addition of 120K at larger molar ratios to actin progressively increases the number of contacts per unit volume and decreases the filament lengths between contacts. The significance of these observations for understanding the mechanism of 120K-mediated gelation is unclear. The 120K protein might bind to and cross-link filaments at only the contact points resulting in a stronger bond between actin filaments than would occur in the absence of 120K. This is consistent with the greater mechanical strength and viscosity [4,25] of actin networks that are formed in the presence of 120K. It would also account for the increase in number of contacts in networks containing more 120K. However, it is not known if the contacts represent sites of specific bonding between filaments mediated by 120K since the location of 120K dimers has not been visualized in our preparations. Certainly, some of the contacts involve interactions between actin filaments alone since such interactions are observed in preparations of pure F actin.

Another possibility is that 120K might bind along the lengths of the filaments without cross-linking them to produce stiff filaments that are less able to slip past each other, thereby causing the network to become rigid. This possibility is consistent with the increase in filament diameter and loss of lateral interactions between filaments observed in preparations containing 120K. It is also consistent with the ability of 120K to inhibit the actin-stimulated Mg ATPase of myosin [4,25]. However, it does not account for the increase in density of contacts observed with increasing molar ratios of 120K dimer:G actin. In all probability, something intermediate between these two possibilities is likely, with 120K being present at some contact points

as well as along the filaments. This discussion serves to emphasize the importance of localizing 120K in these networks.

The increases in network density observed with increasing molar ratios of 120K dimer:G actin could result from the gathering of a constant number of actin filaments into a smaller volume as the number of 120K-mediated cross-links is increased. This would also decrease the filament length between contacts as observed in preparations that contain more 120K. If this possibility were correct, 120K should cause syneresis of solutions of F actin. This has not been tested for 120K, but smooth-muscle filamin has been implicated in the ATP-independent syneresis of solutions of F actin [39].

It is interesting to compare the morphology of 120K-actin networks to networks prepared from macrophage actin-binding protein and actin [35]. Both networks are very similar in appearance and have filaments that converge toward X- or T-shaped contacts. Both networks show increases in density as the amount of respective actin-binding protein is increased relative to actin. Both macrophage actin-binding protein and 120K appear to branch actin filaments when actin is polymerized in their presence [3,11].

These similarities suggest that the ability to form networks of branched filaments may not be the exclusive property of filaminlike proteins since 120K does not resemble filamin or macrophage actin-binding protein in its physical properties [25]. Further comparison of the network-forming properties of these two classes of proteins must await the localization of these proteins in artificial networks and in cells.

Our study of the ultrastructure of critical-point-dried gels reconciles the fact that they are composed of F actin with their amorphous appearance in thin section [5]. Figure 8 is a good illustration of the difficulties encountered when using conventional thin sections to study actin gels. Limited section thickness and the inability to increase the contrast of the specimen above the electron-scattering of the resin give the gel a discontinuous and amorphous appearance. Thus, critical-point drying, freeze drying, or fast-freeze deep etching of whole-mount gels are preferable alternatives for viewing actin networks in three dimensions.

The Cortical Network in Nonextracted Amoeboid Cells

Amoeboid cells of *Dictyostelium discoideum* contain an elaborate filament network that extends from the plasma membrane, where it is present in high density back into the cytoplasm. This network in *Dictyostelium* resembles the cytoplasmic matrix observed in critical-point-dried cultured cells [28,29] and resinless sections of cells cut from solid tissues [26,27].

Since the cells and gels used in this study were chemically fixed in preparation for viewing in HVEM, the possibility that the morphologies of filament networks, observed in situ and in vitro, are artifacts of chemical fixation, must be considered. With regard to the morphology of actin gels in vitro, we have demonstrated that the morphology and density of the gel is a function of the molar ratio of 120K to actin. Furthermore, the presence of a network is demonstrated in 120K-actin gels that have been negative stained without chemical fixation [3]. Finally, it has been possible to generate a dense network with contacts between convergent filaments only with actin and an actin-binding protein. Attempts to generate this morphology by the chemical fixation of concentrated protein solutions of various types [29] or purified F actin alone have failed.

With regard to the presence of networks in situ, filament networks similar to those shown in *Dictyostelium* amoebae are observed routinely in detergent-extracted quick-frozen cells [12], nonextracted quick-frozen, frozen-dried cells [21], frozen, freeze-substituted, and critical-point-dried cells [8], and detergent-extracted, fixed and thin-sectioned [32], or negative-stained cells [13].

There are several lines of evidence that the dense network observed in the cell cortex and its associated structures, such as ruffles and pseudopods, is composed of a complex of 120K and actin. First, most of the filaments comprising the cortical network are actin-containing filaments as demonstrated by the S1 decoration technique [38]. In addition, 120K protein is concentrated in the cell cortex [6,34], particularly in regions containing filament networks [40]. Finally, the cortical network in situ resembles that found in 120K-rich cell extracts.

It should be noted, however, that the cortical network in situ resembles more closely networks formed in 120K-rich extracts than networks assembled in mixtures of purified 120K and actin. The heterogeneity of filament diameters and variation of network density are properties shared by extracts and the cytomatrix in situ, while networks found in purified 120K-actin gels have filament diameters and densities that are more uniform. These differences are certainly due to the more complex composition of cell extracts and cortical cytoplasm as compared to that of purified 120K-actin gels. These reults are consistent with the complex behavior of cell extract SB in response to Ca^{2+}, pH, temperature, and ATP as compared to the immutable gels formed from purified 120K and actin [4,5].

Possible Functions of the Cortical Actin Network in Amoeboid Cells

It is likely that regions of the cell cortex that are rich in 120K and actin are gelled since a gel is formed in vitro at molar ratios of 120K dimer to G actin as low as 1/80 [4,25] while 120K is present in *Dictyostelium* amoebae in amounts sufficient to achieve molar ratios of 1/25 [25]. The gels in situ are likely to have mechanical properties that are similar to 120K-actin gels in vitro since both have the same basic organization, that of a filament network. Finally, the concept that the cortical network represents a gelled state of cytoplasm is consistent with a significant body of evidence that the cytoplasm of amoeboid cells, particularly the cell cortex and its asssociated structures, is capable of dramatic sol-gel transformations [24].

A potentially important consequence of the formation of a 120K-actin network in situ is the effect of 120K on the interaction between actin and myosin. The 120K protein inhibits the actin-stimulated Mg ATPase of myosin in vitro [4,25]. This observation suggests that regions of the cortical network that are rich in 120K would be less likely to participate in actomyosin-dependent motility and that the interaction between 120K and actin may have to be disrupted in order for actin-myosin interactions to occur. This hypothesis is supported by the observation that 120K is excluded from Con A caps, a region of the cell cortex that is rich in actomyosin [2,34].

The presence of numerous attachments between actin filaments in the cortical network and the cell membrane [38] (Fig. 10) indicates that the cortical network is bonded to the cytoplasmic surface of the cell membrane. This fact, combined with the properties of the 120K-actin gel discussed above, suggest that the cortical network could function to freeze cell shape and surface contour, inhibit the lateral mobility of components in the plane of the membrane, and prevent incursion into the cortex of large organelles from the cytoplast.

ACKNOWLEDGMENTS

This work was supported by GM25813 from NIH and a Hirschl Career Scientist Award.

REFERENCES

1. Byers HR, Fujiwara K: J Cell Biol 93:804, 1982.
2. Condeelis J: J Cell Biol 80:751, 1979.
3. Condeelis J: In Schweiger H (ed): "International Cell Biology." Heidelberg: Springer, 1981, pp 306–320.
4. Condeelis J, Geosits S, Vahey M: Cell Motil 2:273, 1982.
5. Condeelis J, Taylor D: J Cell Biol 74:901, 1977.
6. Condeelis J, Salisbury J, Fijiwara K: Nature 292:161, 1981.
7. Condeelis J, Vahey M: J Cell Biol 94:466, 1982.
8. Bridgman P, Reese T: J Cell Biol 99:1655, 1984.
9. Goldman RD, Yerna MJ, Schloss JA: J Supramol Struct 5:155, 1976.
10. Guatelli JC, Porter KR, Anderson KL, Boggs DP: Biol Cell 43:69, 1982.
11. Hartwig J, Tyler J, Stossel T: J Cell Biol 87:841, 1980.
12. Heuser J, Kirschner M: J Cell Biol 86:212, 1980.
13. Small JV: J Cell Biol 91:695, 1981.
14. Ishikawa HR, Bischoff R, Holtzer H: J Cell Biol 43:312, 1969.
15. Kane R: J Cell Biol 71:704, 1976.
16. Lazarides EK, Weber K: Proc Natl Acad Sci USA 71:2268, 1974.
17. Loomis W: Exp Cell Res 64:484, 1971.
18. Luby M, Porter KR: Cell 21:13, 1980.
19. McLean-Fletcher S, Pollard T: J Cell Biol 85:414, 1980.
20. Pollard T: J Cell Biol 68:579, 1976.
21. Porter KR, Anderson KL: Eur J Cell Biol 29:83, 1982.
22. Spudich J, Watt S: J Biol Chem 246:4866, 1971.
23. Stossel T, Hartwig J: J Cell Biol 68:602, 1976.
24. Taylor D, Condeelis J: Int Rev Cytol 56:57–142, 1979.
25. Condeelis J, Vahey M, Carboni J, Demey J, Ogihara S: J Cell Biol 99:119s, 1984.
26. Wolosewick JJ: J Cell Biol 86:675, 1980.
27. Wolosewick JJ, Becker RP, Condeelis JS: In DeBrabander M, DeMey J (eds): "Microtubules and Microtubule Inhibitors." Amsterdam: Elsevier-North Holland, 1980, pp 3–16.
28. Wolosewick JJ, Porter KR: Am J Anat 147:303, 1976.
29. Wolosewick JJ, Porter KR: J Cell Biol 82:114, 1979.
30. Wolosewick JJ, Porter KR: In Maramorsch K and Hirumi H (eds): "Practical Tissue Culture Applications." New York: Academic Press, 1979, pp 59–85.
31. Wong AJ, Pollard TD, Herman IM: Science 219:867, 1983.
32. Schliwa M, Van Blerkom J: J Cell Biol 90:222, 1981.
33. Weeds L: Nature 296:811, 1982.
34. Carboni JM, Condeelis J: J Cell Biol 100:1884–1893.
35. Niederman R, Amreins PC, Hartwig J: J Cell Biol 96:1400, 1983.
36. In Porter K (ed): "The Cytoplasmic Matrix and the Integration of Cellular Function." J Cell Biol 99:(1 Part 2), 1984.
37. Hock R, Condeelis J: Biophys J 47:118a, 1985.
38. Bennett H, Condeelis J: J Cell Biol 99:1434, 1984.
39. Wang K, Singer SJ: Proc Natl Acad Sci USA 74:2021, 1977.
40. Ogihara S, Condeelis J: J Cell Biol 97:270a, 1983.